

# Mass Spectrometric Interrogation of Earwax: Toward the Detection of Ménière's Disease

Allix Marie Coon, Gavin Setzen, and Rabi Ann Musah\*

Cite This: *ACS Omega* 2023, 8, 27010–27023

Read Online

ACCESS |



Metrics &amp; More

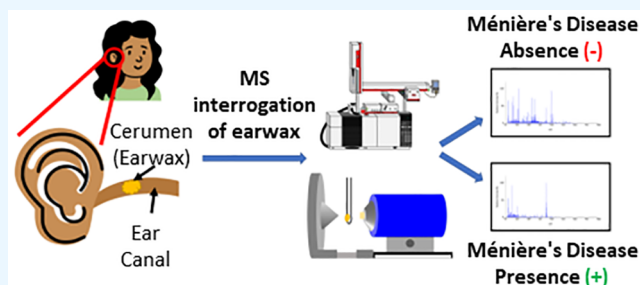


Article Recommendations



Supporting Information

**ABSTRACT:** Many diseases remain difficult to identify because the occurrence of characteristic biomarkers within traditional matrices such as blood and urine remain unknown. Disease diagnosis could, therefore, benefit from the analysis of readily accessible, non-traditional matrices that have a high chemical content and contain distinguishing biomarkers. One such matrix is cerumen (i.e., earwax), whose chemical complexity can pose challenges when analyzed by conventional methods. A combination of cerumen chemical profiles analyzed by gas chromatography–mass spectrometry (GC–MS) and direct analysis in real time—high-resolution mass spectrometry (DART–HRMS) were investigated to ascertain the possible presence of the rare otolaryngological disorder Ménière's disease. This illness is currently identified via “diagnosis by exclusion” in which the disease is distinguished from others with overlapping symptoms by the process of elimination. GC–MS revealed a chemical profile difference between those with and without a Ménière's disease diagnosis by a visually apparent diminution of the compounds present in the Ménière's disease samples. DART–HRMS revealed that the two classes could be differentiated using three fatty acids: *cis*-9-hexadecenoic acid, *cis*-10-heptadecenoic acid, and *cis*-9-octadecenoic acid. These compounds were subsequently quantified by GC–MS and overall, the amounts of these fatty acids were decreased in Ménière's disease patients. The average levels for non-Ménière's disease samples were 7.89  $\mu\text{g}/\text{mg}$  for *cis*-9-hexadecenoic acid, 0.87  $\mu\text{g}/\text{mg}$  for *cis*-10-heptadecenoic acid, and 4.94  $\mu\text{g}/\text{mg}$  for *cis*-9-octadecenoic acid. The average levels for Ménière's disease samples were 1.70  $\mu\text{g}/\text{mg}$  for *cis*-9-hexadecenoic acid, 0.13  $\mu\text{g}/\text{mg}$  for *cis*-10-heptadecenoic acid, and 2.07  $\mu\text{g}/\text{mg}$  for *cis*-9-octadecenoic acid. The confidence levels for *cis*-9-hexadecenoic acid, *cis*-10-heptadecenoic acid, and *cis*-9-octadecenoic acid were 98.7%, 99.9%, and 95.4%, respectively. The results suggest that assessment of the concentrations of these fatty acids could be a useful clinical tool for the more rapid and accurate detection of Ménière's disease.



## INTRODUCTION

Mass spectrometry holds tremendous promise not only as a clinical tool for the routine diagnosis of disease but also for the discovery of disease biomarkers.<sup>1,2</sup> Examples of the increasing use of mass spectrometry in the clinic include detection of vitamin D deficiencies,<sup>3,4</sup> bacterial infection,<sup>4,5</sup> thyroid disease,<sup>1,4</sup> and some cancers.<sup>6</sup> Currently, one of the most widely accepted clinical uses of mass spectrometry is the newborn bloodspot screening for metabolic disorders including but not limited to amino acid, acylcarnitine, and fatty acid oxidation dysregulation disorders; organic acidemias; and hemoglobinopathies.<sup>1,7</sup>

Among the classes of illnesses that have not benefited as much from the use of this technology are otolaryngologic diseases that include functional disorders that affect speaking, swallowing, and hearing, among other activities. Ménière's disease is a case in point. It is a chronic, debilitating, and incurable vestibular disorder that is characterized by a recurring set of symptoms that are believed to be the result of abnormally large amounts of endolymph in the inner ear.<sup>8</sup> Its manifestations include unpredictable recurrent episodes of

vertigo, tinnitus, imbalance, nausea and/or vomiting, a feeling of fullness or pressure in the ear, and fluctuating, progressive low-frequency hearing loss.<sup>9–11</sup> Ménière's disease diagnosis involves the painstaking process of excluding other diseases with overlapping symptoms. As a consequence, the diagnostic workup, which is costly and relies on a combination of patient-reported anecdotes about the episodic experience of symptoms,<sup>12</sup> the results of MRI screenings,<sup>13–16</sup> and balance and hearing tests,<sup>12,17</sup> can yield results that are far from conclusive.<sup>18</sup> For this reason, alternative approaches to disease diagnosis that utilize molecular biomarkers in traditional biological matrices continue to be explored.<sup>19</sup> Promising findings that could, in principle, serve as a basis for disease

Received: March 22, 2023

Accepted: June 16, 2023

Published: July 21, 2023



diagnosis include the depletion of several proteins in blood derived from Ménière's disease patients;<sup>20</sup> the presence of immunoglobulins in the endolymphatic sac luminal fluid, in addition to increased amounts of circulating antibodies;<sup>21</sup> and the presence of miRNAs that are believed to regulate cochlear genes and inflammatory and/or autoimmune pathways.<sup>22</sup> However, there exist a number of challenges to the exploitation of these observations for disease diagnosis. The problem with using peripheral blood is that the collection is not practical and must occur during surgery. With regard to the finding that the blood labyrinthine barrier shows capillary alterations in Ménière's disease patients in contrast to those of controls, the samples were acquired from the cochlea of deceased individuals, and diagnosis using this observation is impractical because this part of the anatomy is not readily accessible antemortem.<sup>23</sup> To circumvent such challenges, the chemical profile of urine as a reporter of the disease has been investigated. It was found that after ingesting mannitol, patients with Ménière's disease exhibited a significant increase in urine volume.<sup>24</sup> However, no insight into the chemical changes associated with the disease was revealed. Thus, it remains highly desirable to identify a readily accessible biological matrix whose chemical makeup can serve as a reporter of Ménière's disease and other relevant neurotological disorders so that more rapid and accurate diagnosis can be achieved based on assessment of the presence, absence, or change in concentrations of relevant compounds.

A number of non-traditional biological matrices such as sweat<sup>25</sup> and saliva<sup>26</sup> are being investigated for their utility as reporters of disease. One such matrix that is receiving increasing attention is cerumen (i.e., earwax),<sup>27–29</sup> a lipid-rich complex mixture comprised of dead skin cells, hair, and various oily secretions produced by the sebaceous and apocrine sweat glands within the ear canal.<sup>30</sup> It contains the most concentrated levels and highest diversity of surface accessible lipids in the human body. There are two types—wet and dry, and the form observed depends on genetics. The type of cerumen produced by an individual is defined by a single nucleotide polymorphism in the ATP-binding cassette C11 gene.<sup>31,32</sup> Dry-type individuals are homozygous for adenine while the wet-type exhibit at least one guanine. Investigations of the molecular content of cerumen have revealed the presence of a number of compound classes such as organic acids,<sup>33–38</sup> amino acids,<sup>34,39</sup> carbohydrates,<sup>40</sup> lipids,<sup>38,41,42</sup> alcohols,<sup>35,37,38</sup> hydrocarbons,<sup>37,38,43</sup> and esters.<sup>37,38</sup> The analysis techniques used include gas chromatography (GC),<sup>35,37</sup> gas chromatography–mass spectrometry (GC–MS),<sup>36,37</sup> pyrolysis GC–MS,<sup>43</sup> two-dimensional GC–MS (GC × GC–MS),<sup>38</sup> column chromatography,<sup>40</sup> paper chromatography,<sup>33,34</sup> and thin layer chromatography.<sup>37,41,42</sup>

Even though cerumen is commonly considered to have little to no clinical relevance, its physical characteristics have been found to be associated with several disorders. For example, an increase in waxy constituents is associated with psoriasis; “scanty” and dry earwax is found in those with cystic fibrosis; dark brown or black earwax occurs with alkaptonuria; and those with Parkinson's disease usually produce an excess of wax that can lead to ear canal blockage.<sup>27</sup> Furthermore, earwax has been shown to contain biomarkers indicative of underlying disease states. The characteristic odor of maple syrup urine disease (MSUD) is detectable in the cerumen of newborns as early as 12 h after birth.<sup>44</sup> However, in general, the aforementioned physical descriptions cannot be used for

definitive diagnosis, and with the exception of MSUD, identification of specific compounds related to these diseases has not been accomplished. In 2017, a pilot study was performed comparing earwax from non-diabetic patients and that from donors with type 1 and type 2 diabetes. Statistically significant variations in the concentrations of volatile biomarkers, which enabled discrimination between healthy, type 1, and type 2 diabetic patients, were observed.<sup>28</sup> It was also found that by using headspace GC–MS, patients with and without a diagnosis of certain cancers (carcinoma, lymphoma, and leukemia) could be differentiated from one another using 27 volatile organic markers. However, further work was needed to discriminate between the various cancers studied.<sup>29</sup> Such findings hint at the possibility that earwax can be used as a disease diagnosis tool and, in principle, novel approaches could be developed using earwax rather than more traditional body fluids, to screen for diseases. In recent years, technological advances that have been made in the areas of ambient ionization mass spectrometry provide unique opportunities for the investigation of complex lipid-rich matrices such as cerumen and to reveal information about their chemical phenotypes that can be exploited for non-invasive disease diagnosis purposes. In this regard, if a “normal” profile of cerumen can be established, there can then be investigations into whether its chemical makeup undergoes changes as a function of different metabolic “states”.<sup>38</sup> These lipid changes could then be correlated to various diseases including, but not limited to, inner ear or neurotological disorders and lead to the development of new, rapid, accurate, and non-invasive testing protocols.

Toward the goal of exploring the utility of cerumen for disease diagnosis, GC–MS and the ambient mass spectrometry technique direct analysis in real time—high-resolution mass spectrometry (DART-HRMS) were investigated in combination. GC–MS was used to assess and identify the potential chemical markers that result in differences between those with and without a diagnosis of Ménière's disease. DART-HRMS enables the rapid analysis of a broad range of complex matrices such as plant material,<sup>45–49</sup> animal tissue,<sup>50–53</sup> food products,<sup>54</sup> items of forensic relevance,<sup>55–57</sup> and even biological matrices such as serum<sup>58,59</sup> and urine.<sup>59–62</sup> This method requires little to no sample preparation steps for qualitative analysis, and samples can be analyzed in their native form. Further, the analysis is rapid and can be completed within only a few seconds. These attributes make it a potentially powerful tool for the routine analysis of earwax. We report herein the application of these two approaches for the analysis of cerumen samples acquired from donors with and without a diagnosis of Ménière's disease. The lipid profiles between the two were observed to be starkly different, and this not only enabled their differentiation, but also revealed aspects of the chemical basis for this discrimination.

## RESULTS AND DISCUSSION

**Mass Spectral Analysis of Earwax.** The focus of this study was to identify possible small-molecule biomarkers of Ménière's disease, revealed by the chemical analysis of cerumen. Because cerumen exhibits high chemical complexity and contains both endogenous and exogenous components that vary depending on donor lifestyle, age, and so forth, the goal was to determine the presence of commonalities across Ménière's disease samples that were independent of the race, sex, body mass index (BMI), the presence of comorbidities, or

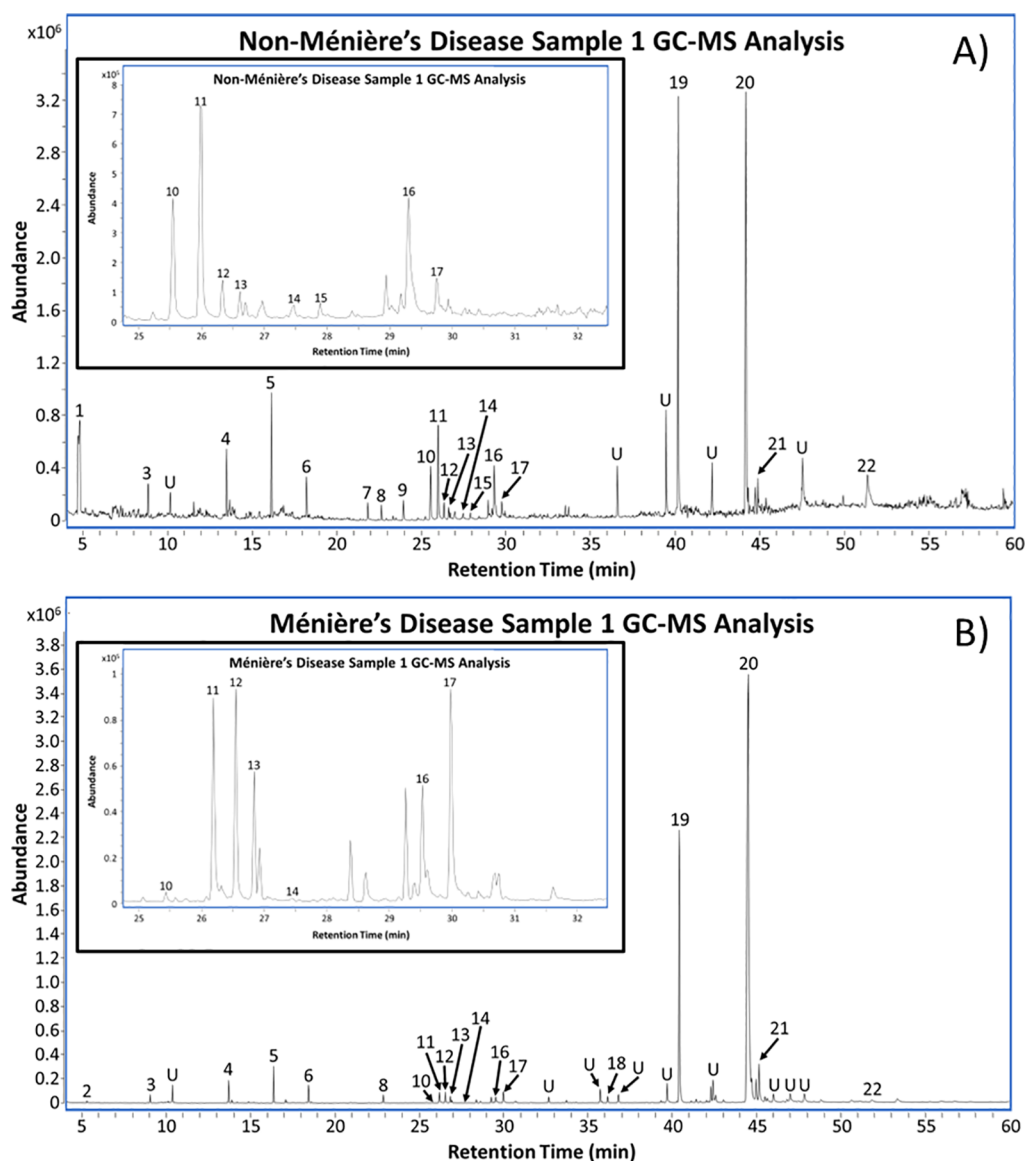


**Figure 1.** Representative gas chromatograms of earwax. Panel A shows a sample from a donor without Ménière's disease and panel B shows a sample from a donor with Ménière's disease. The identities of the numbered peaks are shown in Table 1. Peaks denoted "U" were not identified. The insets highlight the area between 25 and 32 min.

lifestyle practices (e.g., personal cleaning of ears or frequent swimming), which contrasted with the chemical signatures of samples from donors who did not have the disease. For this reason, samples were disaggregated into two classes only, purely on the basis of whether or not the donor received a diagnosis of Ménière's disease.

To determine whether the chemical profiles of the Ménière's disease and non-Ménière's disease samples exhibited intra-class consistencies and inter-class differences, the chemical profiles of both sample types were first surveyed by gas chromatography–mass spectrometry (GC–MS). In previous work, it was determined through iterative mass spectrometric analyses of "bulk" cerumen (consisting of plugs from multiple donors) as a function of its suspension in different solvents that ethyl acetate solubilizes the greatest number and broadest range of compounds,<sup>38</sup> and for this reason, ethyl acetate was used for the extractions that were analyzed here. Samples for this work were derived from multiple donors as plugs, with each plug representing a single individual. Representative gas chromatograms

illustrative of the results of these analyses are presented in Figure 1, with the insets showing a magnification of the chromatograms between 25 and 32 min. Panel A shows the results from a non-Ménière's disease donor, and panel B shows the results from a donor with a diagnosis of Ménière's disease. The identities of the numbered peaks, which were assigned based on retention times, mass spectral electron ionization (EI) fragmentation pattern matching, and comparisons to the retention times and fragmentation patterns of authentic standards, are listed in Table 1. In Table 1, "X" denotes the detection of the indicated compound in the Ménière's disease or non-Ménière's disease cerumen sample, and an asterisk (\*) indicates exogenous compounds introduced from the environment such as the ubiquitous phthalate plasticizer, bis(2-ethylhexyl) phthalate. The results presented in Table 1 also indicate that while most of the identified compounds were detected in both sample classes, a few were not shared. For example, while 1-decene appeared in the Ménière's disease sample, it was absent in the non-Ménière's disease sample.

**Table 1. Compounds Detected by GC–MS Analysis of Ethyl Acetate Extracts of Earwax Plugs Derived from Individual Ménière's Disease and Non-Ménière's Disease Donors<sup>a,b</sup>**

Peak number	Compound identity	Non-Ménière's disease sample 1	Ménière's disease sample 1
1	glycerin	X	—
2	1-decene	—	X
3	1-dodecene	X	X
4	1-tetradecene	X	X
5*	2,4,-di- <i>tert</i> -butylphenol	X	X
6	1-hexadecene	X	X
7	tetradecanoic acid	X	—
8	1-octadecene	X	X
9	pentadecanoic acid	X	—
10	<i>cis</i> -9-hexadecenoic acid	X	X
11	hexadecanoic acid	X	X
12*	3,5-di- <i>tert</i> -butyl-4-hydroxyphenylpropionic acid	X	X
13*	benzenepropanoic acid, 3,5-bis(1,1-dimethylethyl)-4-hydroxy-, ethyl ester	X	X
14	<i>cis</i> -10-heptadecenoic acid	X	X
15	heptadecanoic acid	X	—
16	<i>cis</i> -9-octadecenoic acid	X	X
17	octadecanoic acid	X	X
18*	bis(2-ethylhexyl) phthalate	—	X
19	squalene	X	X
20	cholesterol	X	X
21	lathosterol	X	X
22	hexadecanoic acid tetradecyl ester	X	X

<sup>a</sup>An “X” indicates that the compound was detected in the sample and a dash (—) indicates that it was not. <sup>b</sup>With the exception of compounds represented by peak numbers 1, 2, 5, 12, 13, 15, and 18, all of the listed compounds were also observed in the previous study reported in ref 38. \*Xenobiotic contaminant.

However, tetradecanoic acid was detected in the non-Ménière's disease sample, but not the Ménière's disease sample. It is important to note that there were some instances where tetradecanoic acid was detected in the Ménière's disease earwax plugs, and 1-decene appeared in the non-Ménière's disease samples. This is illustrated in the additional chromatograms representative of the earwax of other Ménière's disease and non-Ménière's disease donors that are presented in Supporting Information Figure S1.

From the chromatograms, a number of trends were apparent. First, all of the molecules observed represented compound classes that have been reported in earlier studies including alkenes,<sup>37,38,43</sup> fatty acids,<sup>33–38</sup> and esters,<sup>37,38</sup> and all the detected exogenous compounds have been previously reported to be in earwax. Second, the chromatograms of both sample types were dominated by the presence of squalene (peak #19) and cholesterol (peak #20), with the areas under the curves (AUCs) being of similar magnitude in both samples. For example, the AUC of squalene (peak #19) in the non-Ménière's disease sample (panel A) was  $9.3 \times 10^6$  and in the Ménière's disease sample (panel B) was  $8.3 \times 10^6$ . The AUC of cholesterol (peak #20) in the non-Ménière's disease sample (panel A) was  $13.1 \times 10^6$  and in the Ménière's disease sample (panel B) was  $28.7 \times 10^6$ . Third, although the chemical profiles of the non-Ménière's disease and Ménière's disease samples were quite similar, it was generally observed that the relative amounts of the molecules present were starkly different, which is readily apparent from visual examination of panels A and B in Figure 1. Relative to squalene and cholesterol, the other peaks in the Ménière's disease chromatogram are diminished in comparison to the chromatogram for the non-Ménière's disease sample. This trend was consistent and can be observed in the other Ménière's disease and non-Ménière's disease

donor chromatograms presented in Supporting Information Figure S1. The identities of some of the peaks in the chromatograms are unknown (labeled “U”). However, even with consideration of these peaks, a fourth observation was that there were no peaks that uniquely appeared in all of the Ménière's disease samples, and which did not appear in the non-Ménière's disease samples. This implied that for the compounds detectable by GC–MS, no Ménière's disease-specific biomarkers were observed.

**DART-HRMS Analysis of Earwax.** Previous work has shown that in contrast to the use of GC–MS for interrogation of complex matrices, analyses by DART-HRMS often reveals a broader range of analytes that span the dielectric constant spectrum, that is inclusive of the compounds detected by GC–MS.<sup>63</sup> To determine whether there were other compounds present, over and beyond those detectable by GC–MS and which were unique to Ménière's disease, earwax was subjected to analysis by DART-HRMS. Earwax samples from fifteen individuals, comprised of seven plugs from donors without Ménière's disease and eight from patients with a confirmed or tentative case of Ménière's disease were analyzed by DART-HRMS. Representative results for DART mass spectral analysis of cerumen plugs from a non-Ménière's disease donor and from a patient with a confirmed case of Ménière's disease are presented in Figure 2 panels A and B, respectively. The numbered peaks correspond to protonated monoisotopic high-resolution masses that were consistent with those of compounds confirmed by GC–MS to be present (see Table 1. For example, the peak labeled #19 in the DART mass spectrum in Figure 2A corresponds to the protonated monoisotopic mass of squalene. Thus, it was observed that there were *m/z* values in the DART mass spectra that were consistent with the masses of compounds detected by GC–

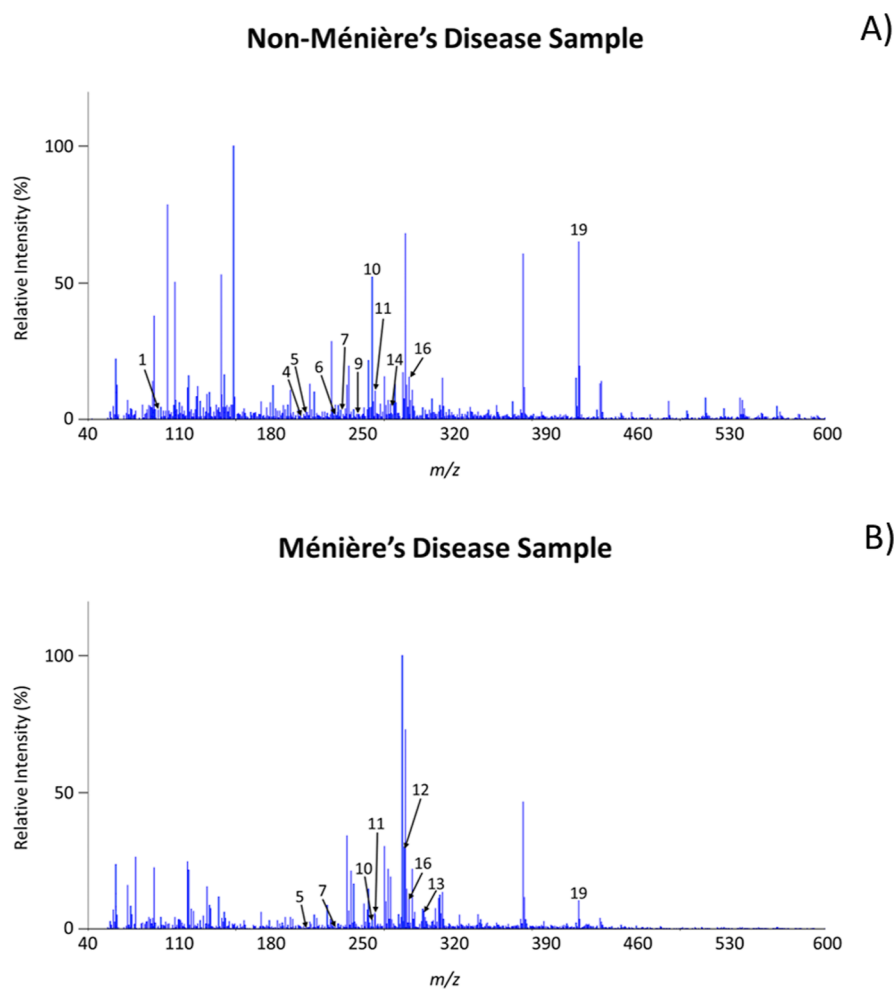


**Figure 2.** Representative DART mass spectra of ethyl acetate extracts of earwax. Panel A shows a sample from a donor without Ménière's disease and panel B shows a sample from a donor with Ménière's disease. The identities of the numbered peaks correspond to those identified by GC–MS and are shown in Table 1.

MS. Not every peak identified by GC–MS was detected in every DART mass spectrum, which is why it is important to analyze multiple replicates of each sample. Every peak that was identified by GC–MS had a corresponding  $m/z$  value detected by DART-HRMS in at least one replicate of each plug analyzed (data not shown). While we detected masses in the DART mass spectra whose identities were consistent with those found by GC–MS, a broader range of  $m/z$  values, over and above those seen in GC–MS, was observed. Presented in Figures 3 and 4 are representative DART mass spectra of ethyl acetate extracts of earwax from non-Ménière's disease and Ménière's disease donors, respectively. Although each of the non-Ménière's disease samples in Figure 3 panels A through F were visually distinct, there were a subset of peaks representing compounds that they had in common. These, which were detected and identified in this work and earlier studies, include hexadecanoic acid, *cis*-9-hexadecenoic acid, *cis*-10-heptadecenoic acid, octadecanoic acid, *cis*-9-octadecenoic acid, squalene, cholesta-3,5-diene, and lanosterol.<sup>38</sup> The chemical distinctions between these samples may be a consequence of differences in diet, lifestyle, age, or even the presence of medications consumed by the individual. For example, in the analysis of some samples, prescription medications such as sildenafil were observed (data not shown). A range of over 1000 compounds have been detected in earwax. Using a 1% relative abundance

threshold cutoff, the number of peaks in the non-Ménière's disease samples ranged from 151 to 775, with the average being 380. This is in stark contrast to the approximately 30 peaks detected by GC–MS and highlights the added benefit of using ambient ionization mass spectrometry as a complementary technique. In contrast to the range of peaks observed in the non-Ménière's disease samples, the Ménière's disease samples exhibited relatively fewer peaks. The average number of peaks in the latter samples was 289, which is ~24% lower than was observed for the non-Ménière's disease samples. This distinction is visually apparent when the spectra shown in Figures 3 and 4 are compared. However, it is important to note the possibility that even though the analyses were conducted under soft ionization conditions, implying that the detected peaks represent protonated precursors of the analytes, the increase in the number of peaks in the non-Ménière's disease samples could be a consequence of the fragmentation of molecules that are unstable under the mild conditions of the experiment. Nevertheless, there was a consistent trend that fewer peaks were observed in the Ménière's disease samples. This is also similar to what was seen in the GC–MS analyses. An implication of this is that the Ménière's disease samples are characterized by a paucity of many of the compounds present in non-Ménière's disease cerumen, even when accounting for the natural intra-sample variation observed. These distinctions

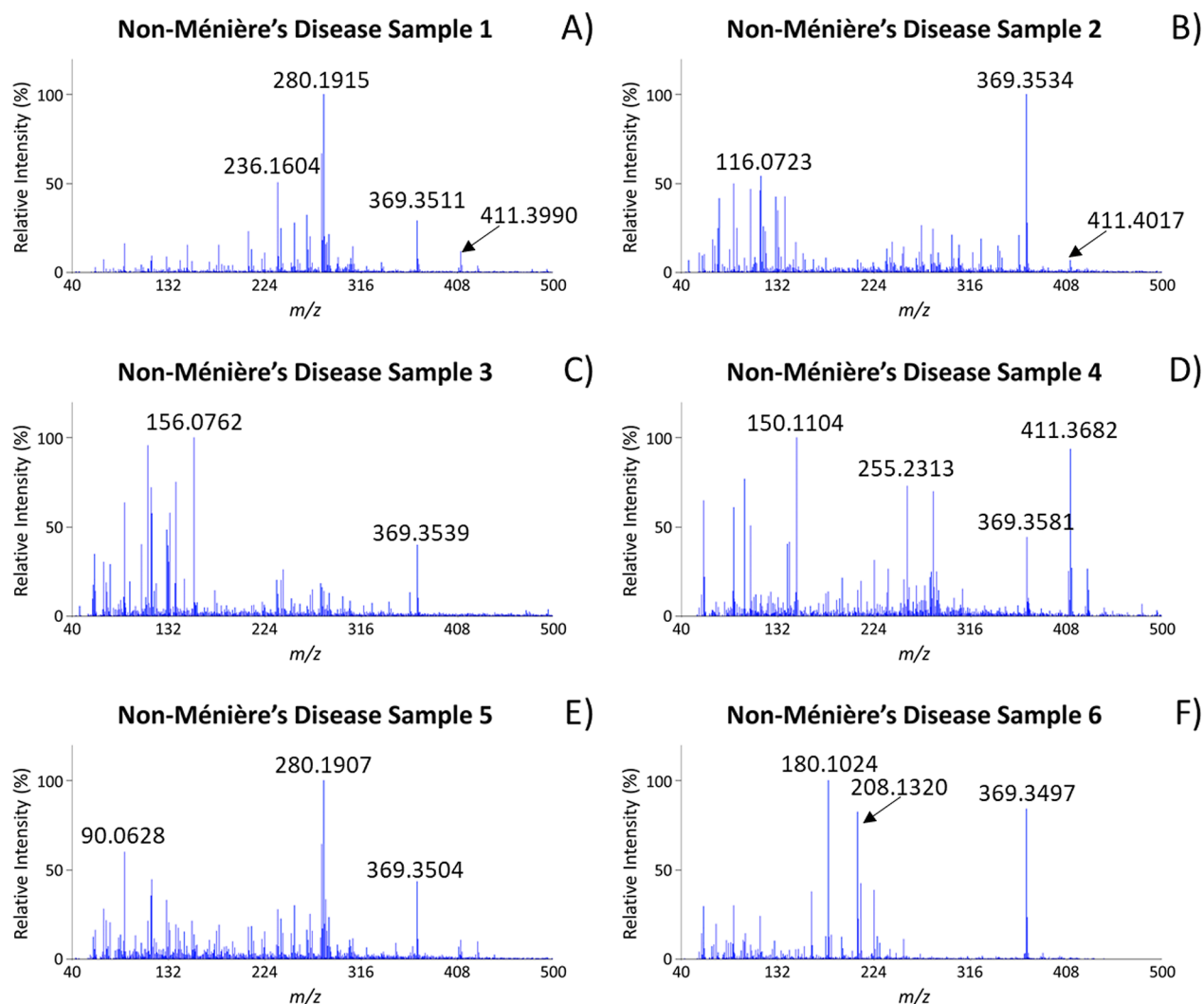


**Figure 3.** Panels A through F show representative DART mass spectra of ethyl acetate extracts of earwax from donors without Ménière's disease. The prominent peaks are labeled, some of which were identified by GC–MS and are reported in Table 2.

between the two sample types were consistently noted in the analyses of all samples.

**Distinguishing between Ménière's Disease and Non-Ménière's Disease Cerumen Samples.** To answer the question of which subset of the broad range of compounds detected had a statistically significant impact on contrasting between the two classes, the DART mass spectral data were subjected to statistical analysis. Six non-Ménière's disease and six Ménière's disease samples were analyzed. While the utilization of a greater number of samples was desirable, the rarity of Ménière's disease greatly reduced the number available. Thus, even though a far greater number of non-Ménière's disease samples were available, the multivariate statistical analysis processing was limited to the inclusion of only six representative spectra, in order to keep the Ménière's disease and non-Ménière's disease data balanced.

To first determine whether the between class variation was significant in comparison with the within class variations, principal component analysis (PCA) and multivariate analysis of variance (MANOVA) were used. The data were scaled using the "autoscaling" function and subjected to PCA to reduce the dimensionality, and 6 principal components were used in the MANOVA analysis. This process uses multiple variables to

estimate the intra- and inter-variation between groups. A  $p$ -value of  $7.98 \times 10^{-5}$  ( $<0.05$ , significance threshold level) was obtained by MANOVA, indicating that although there were variations within the mass spectra of the non-Ménière's disease class, and also within the Ménière's disease class samples, the differences between the two classes were statistically significant.

Based on the MANOVA results showing that the DART mass spectra from non-Ménière's disease and Ménière's disease donors do exhibit distinct chemical profiles, multivariate statistical analysis was performed. Accordingly, the technique random forest (RF) was applied to the mass spectral data to investigate this trend and identify which  $m/z$  values were predictors of Ménière's disease. A heatmap rendering of the mass spectral data was first generated. From the heatmap rendering, the masses-to-feature selection tool in the Mass Mountaineer software was utilized with a bin width of  $\pm 5$  millimass units (mmu) and a relative abundance threshold cutoff of 2% to reveal the masses that were most heavily weighted in facilitating differentiation between the two classes. An iterative process was then employed to reveal the subset of masses that enabled the accurate prediction of the presence of Ménière's disease. The RF model exhibited a prediction error

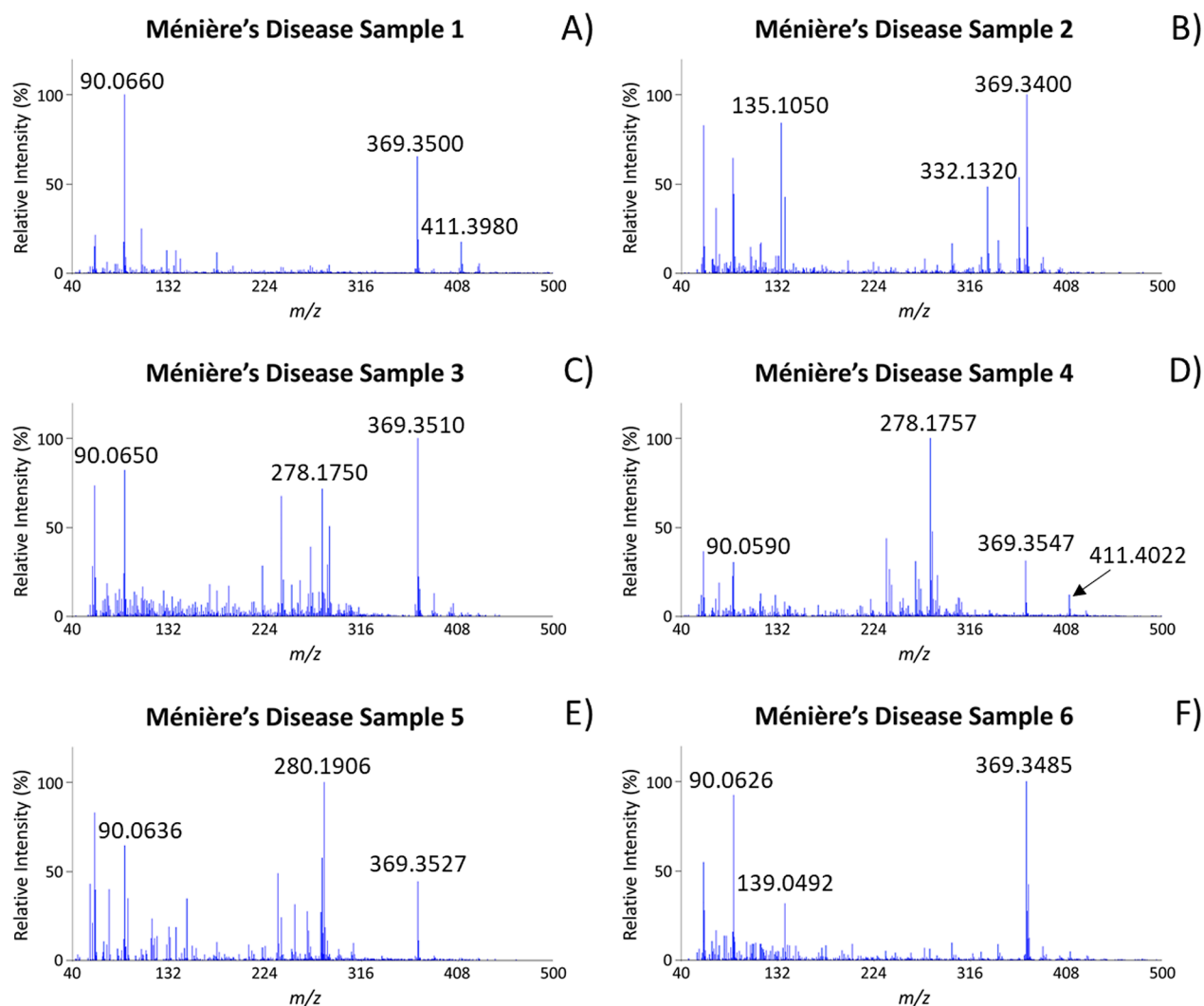


**Figure 4.** Panels A through F show representative DART mass spectra of ethyl acetate extracts of earwax from donors with Ménière's disease. The prominent peaks are labeled, some of which were identified by GC–MS and are reported in Table 3.

of 0.2583 with modest internal classification merits (accuracy, sensitivity, and precision) (see Supporting Information Table S13). Nevertheless, from this treatment, three masses emerged as optimal for the discrimination between the two classes: 255.2324, 269.2481, and 283.2637. These protonated mono-isotopic masses correspond to the formulas  $C_{16}H_{30}O_2$ ,  $C_{17}H_{32}O_2$ , and  $C_{18}H_{34}O_2$  and are consistent with those of three fatty acids confirmed to be present in the cerumen samples by GC–MS analysis and comparison to authentic standards, namely: *cis*-9-hexadecenoic acid, *cis*-10-heptadecenoic acid, and *cis*-9-octadecenoic acid, respectively (appearing in the 25 to 30 min retention time region of the chromatograms).

To assess the ability of the RF model to accurately predict the class of samples that were not included in the creation of the model itself, three external samples were screened against it: one from a donor without Ménière's disease, one from a patient with a confirmed Ménière's disease diagnosis, and one from a patient with a tentative diagnosis of Ménière's disease. Ethyl acetate extracts of these samples, prepared in a manner similar to that used to build the model, were each analyzed in replicates of ten. Figure 5 shows a representative spectrum for each of these samples, and the mass data tables associated with

these spectra are presented in Supporting Information Tables S14 through S16. The identities of the numbered peaks correspond to those identified by GC–MS and are shown in Table 1. The peak corresponding to cholesta-3,5-diene is also labeled. The model was found to be 100% accurate for predicting the class of the external validation samples. The prediction results are summarized in Supporting Information Table S17. The results indicate that: (1) it is highly probable that the patient who received a tentative diagnosis of Ménière's disease does in fact have the disorder, given that the sample was classified as Ménière's disease by the RF model. This is supported by the appearance of fewer peaks relative to the large number of peaks visually observed in the spectra of the non-Ménière's disease samples in Figure 3; and (2) the most likely reason that the external validation results were highly accurate while the classification merits of the RF model were low was due to the intra-sample variation between earwax plugs that were members of the same class, as previously described. Although the internal classification results were only modestly accurate, the RF analysis affirmed the utility of the subset of the three fatty acids in enabling discrimination between Ménière's disease and non-Ménière's disease samples. In this regard, it was noted that the success in discriminating

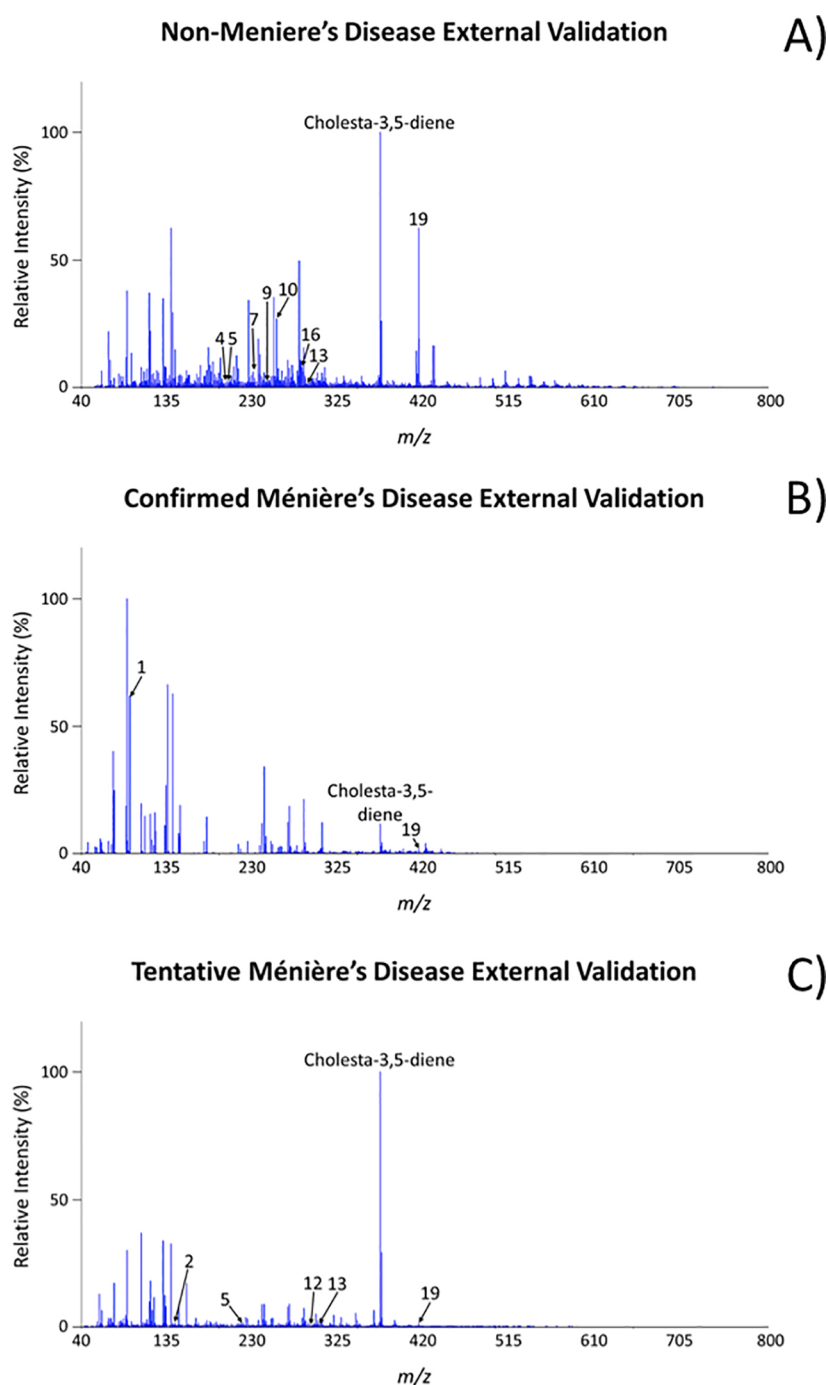


**Figure 5.** Representative mass spectra of the earwax analyzed by DART-HRMS in positive-ion mode and screened against the developed statistical model. Panel A represents earwax from a donor without Ménière's disease; panel B represents earwax from a donor with a confirmed case of Ménière's disease; and panel C represents earwax from a donor with a tentative diagnosis of Ménière's disease. The identities of the numbered peaks correspond to those identified by GC-MS and are shown in Table 1. The compound cholesta-3,5-diene is also labeled.

between the two classes was not a consequence of the presence or absence of the fatty acid biomarkers, but rather a result of the consistently observed lowered ion counts for these compounds in the mass spectra of the earwax of Ménière's disease donors versus that in the earwax of donors who did not have the disease. Thus, to assess this further, their levels in Ménière's disease and non-Ménière's disease samples were quantified.

**Quantification of Fatty Acids.** To assess whether there were differences in the concentrations of the three fatty acids

that appeared to be important in differentiating Ménière's disease and non-Ménière's disease samples, the levels of *cis*-9-hexadecenoic acid, *cis*-10-heptadecenoic acid, and *cis*-9-octadecenoic acid in the two classes of samples were quantified. Nine non-Ménière's disease samples were used, as well as six Ménière's disease plugs (from 15 individuals in total). The number of Ménière's disease samples was limited due to disease rarity, but additional non-Ménière's disease plugs were used to ensure broader representation of samples. In these studies, 19-methyl eicosanoic acid was used as an

**Table 2. Protonated, Monoisotopic Masses Detected in the DART Mass Spectra of the Non-Ménière's Disease Samples That Were Consistent with Those of Compounds That Were Identified in This Work by GC-MS<sup>a</sup>**

Compound	Protonated monoisotopic mass	Non-Ménière's disease sample 1	Non-Ménière's disease sample 2	Non-Ménière's disease sample 3	Non-Ménière's disease sample 4	Non-Ménière's disease sample 5	Non-Ménière's disease sample 6
glycerin	93.0552	—	93.0554	93.0587	93.0611	—	—
1-decene	141.1643	—	141.1619	—	—	—	—
1-tetradecene	197.2269	—	—	197.2248	—	—	—
2,4,-di- <i>tert</i> -butylphenol	207.1749	207.1663	207.1743	—	207.1802	207.1677	—
1-hexadecene	225.2582	—	—	—	225.2671	—	—
tetradecanoic acid	229.2168	229.2112	—	—	229.2157	—	—
pentadecanoic acid	243.2324	243.2252	—	—	243.2283	—	—
<i>cis</i> -9-hexadecenoic acid	255.2324	255.2309	—	—	225.2313	—	—
hexadecanoic acid	257.2481	—	—	—	257.2495	—	—
3,5-di- <i>tert</i> -butyl-4-hydroxyphenylpropionic acid	279.1960	279.1951	—	279.2020	—	279.1942	—
benzene propanoic acid, 3,5-bis(1,1-dimethylethyl)-4-hydroxy-, ethyl ester	293.2117	293.2210	—	293.2104	—	293.2194	—
<i>cis</i> -10-heptadecenoic acid	269.2481	—	—	—	269.2422	—	269.2530
<i>cis</i> -9-octadecenoic acid	283.2637	—	—	—	283.2661	—	283.2629
octadecanoic acid	285.2794	—	—	—	—	—	285.2749
squalene	411.3991	411.3990	411.4017	411.4025	411.3982	411.3984	411.4038
cholesterol	387.3627	—	387.3570	—	—	—	387.3656
lathosterol	387.3627	—	387.3570	—	—	—	387.3656
hexadecanoic acid tetradecyl ester	453.4672	—	—	—	—	453.4729	—

<sup>a</sup>A dash (—) indicates that the mass was not detected within the specific replicate that was analyzed (using a mass tolerance of  $\pm 10$  muu).

**Table 3. Protonated, Monoisotopic Masses Detected in the DART Mass Spectra of the Ménière's Disease Samples That Were Consistent with Those of Compounds That Were Identified in This Work by GC-MS<sup>a</sup>**

Compound	Protonated monoisotopic mass	Ménière's disease sample 1	Ménière's disease sample 2	Ménière's disease sample 3	Ménière's disease sample 4	Ménière's disease sample 5	Ménière's disease sample 6
glycerin	93.0552	—	—	—	—	93.0560	—
1-dodecene	169.1956	—	169.1940	—	—	—	—
2,4,-di- <i>tert</i> -butylphenol	207.1749	207.1730	207.1690	207.1730	207.1731	—	207.1689
1-hexadecene	225.2582	—	—	225.2550	—	—	—
tetradecanoic acid	229.2168	—	—	229.2150	229.2157	229.2215	—
<i>cis</i> -9-hexadecenoic acid	255.2324	255.2310	—	255.2320	255.2322	—	—
hexadecanoic acid	257.2481	—	—	257.2460	257.2461	—	—
3,5-di- <i>tert</i> -butyl-4-hydroxyphenylpropionic acid	279.1960	279.1950	—	—	279.1913	279.1972	—
benzene propanoic acid, 3,5-bis(1,1-dimethylethyl)-4-hydroxy-, ethyl ester	293.2117	293.2150	293.2100	293.2110	293.2180	—	—
<i>cis</i> -9-octadecenoic acid	283.2637	283.2630	—	—	283.2667	—	—
bis(2-ethylhexyl) phthalate	391.2848	—	—	—	—	—	391.2902
squalene	411.3991	411.3980	—	411.3990	411.4022	411.4017	411.4016
cholesterol	387.3627	387.3690	387.3720	387.3580	387.3545	387.3593	—
lathosterol	387.3627	387.3690	387.3720	387.3580	387.3545	387.3593	—
hexadecanoic acid tetradecyl ester	453.4672	453.4720	—	—	—	—	—

<sup>a</sup>A dash (—) indicates that the mass was not detected within the specific replicate that was analyzed (using a mass tolerance of  $\pm 10$  muu).

**Table 4. Average Concentrations of the Indicated Fatty Acids in Non-Ménière's Disease and Ménière's Disease Samples of Earwax, and the Calculated Confidence Level for Each**

Sample class and confidence level	<i>cis</i> -9-Hexadecenoic acid	<i>cis</i> -10-Heptadecenoic acid	<i>cis</i> -9-Octadecenoic acid
non-Ménière's disease average concentration	7.89 $\mu\text{g}/\text{mg}$	0.87 $\mu\text{g}/\text{mg}$	4.94 $\mu\text{g}/\text{mg}$
Ménière's disease average concentration	1.70 $\mu\text{g}/\text{mg}$	0.13 $\mu\text{g}/\text{mg}$	2.07 $\mu\text{g}/\text{mg}$
Confidence level	98.7%	99.9%	95.4%

internal standard. Since this analysis was targeted to detection of fatty acids specifically, hexanes solvent was used in order to

maximize their extraction, and a fatty acid specific GC column (HP-FFAP) was used for their detection. A representative

standard curve developed for the quantification experiment is shown in Supporting Information Figure S2, and the quantification results are presented in Supporting Information Table S18. An entry of 0 indicates that the fatty acid was not detected. In some instances, the fatty acid was detected but the concentration was below the quantification limit and is denoted “BQL”. For the non-Ménière’s disease samples, the average concentrations were as follows: *cis*-9-hexadecenoic acid, 7.89  $\mu\text{g}/\text{mg}$ ; *cis*-10-heptadecenoic acid, 0.87  $\mu\text{g}/\text{mg}$ ; and *cis*-9-octadecenoic acid, 4.94  $\mu\text{g}/\text{mg}$ . For the Ménière’s disease samples, the average concentrations were: *cis*-9-hexadecenoic acid, 1.70  $\mu\text{g}/\text{mg}$ ; *cis*-10-heptadecenoic acid, 0.13  $\mu\text{g}/\text{mg}$ ; and *cis*-9-octadecenoic acid, 2.07  $\mu\text{g}/\text{mg}$ , and these values are reported in Table 4. Overall, it was found that compared to the non-Ménière’s disease samples, the Ménière’s disease samples showed a marked decrease in the concentrations of these three fatty acids of  $\sim 78.4\%$ ,  $85.3\%$ , and  $58.2\%$ , respectively. Determination of the strength of each of these fatty acid variables in enabling differentiation of the two sample types (i.e., the confidence level) was performed using a *T*-test. The confidence levels were computed to be: 98.7% for *cis*-9-hexadecenoic acid; 99.9% for *cis*-10-heptadecenoic acid; and 95.4% for *cis*-9-octadecenoic acid (presented in Table 4). The observation that the confidence levels for all three fatty acids were above 90% indicates that their ability to enable differentiation of the two sample classes is statistically significant.

To determine whether the levels of the fatty acids in the correctly classified external validation samples in Figure 5 aligned with the trends observed in the Ménière’s disease and non-Ménière’s disease control samples (i.e., lower levels of fatty acids in the former compared to the latter), the quantification of the fatty acids in the external validation samples was also performed. The quantification results are shown in Supporting Information Table S19. For the external validation non-Ménière’s disease sample, the amounts of *cis*-9-hexadecenoic acid, *cis*-10-heptadecenoic acid, and *cis*-9-octadecenoic acid were 19.12, 1.91, and 12.62  $\mu\text{g}/\text{mg}$ , respectively. These values are all above the average concentration for these fatty acids in non-Ménière’s disease samples. For the external validation tentative Ménière’s disease sample, the concentrations of *cis*-9-hexadecenoic acid, *cis*-10-heptadecenoic acid, and *cis*-9-octadecenoic acid were 2.12, 0.48, and 11.49  $\mu\text{g}/\text{mg}$ , respectively. The values of *cis*-9-hexadecenoic acid and *cis*-10-heptadecenoic acid were slightly above the average value typical for Ménière’s disease but lower than the average values for non-Ménière’s disease. The value of *cis*-9-octadecenoic acid was much higher than even the non-Ménière’s disease average. For the external validation-confirmed Ménière’s disease sample, the *cis*-9-hexadecenoic acid, *cis*-10-heptadecenoic acid, and *cis*-9-octadecenoic acid concentrations were 7.56, 0.72, and 2.40  $\mu\text{g}/\text{mg}$ , respectively. The concentrations of *cis*-10-heptadecenoic acid and *cis*-9-octadecenoic acid were just above the average that was typical for Ménière’s disease samples. However, they were lower than the average calculated values of the non-Ménière’s disease samples for those specific fatty acids. The concentration of *cis*-9-hexadecenoic acid aligned more with the average concentration of the non-Ménière’s disease sample. The results illustrate that it is important to not only consider the concentration levels of all three of these fatty acids together but to also consider the concentration range for each in making an assessment of Ménière’s disease. This variability could be a

consequence of concentrations of fatty acids that occur on a continuum that reflects disease progression, the lower concentrations being observed with more advanced stages. The study of the progression of Ménière’s disease as a function of the concentration of these fatty acids is the focus of ongoing work. While we were able to identify a combination of three fatty acids, the relative concentrations of which could be used to predict the presence of Ménière’s disease, it remains unknown why the levels of these three particular fatty acids serve as disease predictors, or whether these fatty acids might also be predictors of other otolaryngological disorders. The etiology of Ménière’s disease remains unknown, but our findings may provide clues about the connection between disease occurrence and lipid dysregulation. These considerations are the subjects of ongoing investigations.

## CONCLUSIONS

For the first time, a chemical basis for the detection of Ménière’s disease has been devised based on the analysis of earwax, a matrix that can be readily and non-invasively collected. The chemical profiles of earwax from donors with and without Ménière’s disease exhibit consistent chemical profile differences that can be revealed by GC–MS and DART-HRMS, and these distinctions can be leveraged to predict disease presence. The application of random forest to the DART-HRMS-derived chemical profiles of earwax provided a non-subjective means to facilitate the differentiation of the two sample types. The *m/z* values that were used as the basis for the ability to discriminate between Ménière’s disease and non-Ménière’s disease classes were determined to be *cis*-9-hexadecenoic acid, *cis*-10-heptadecenoic acid, and *cis*-9-octadecenoic acid. Quantification of their amounts within the two sample classes revealed that their levels in the Ménière’s disease samples were lower by 58.2–85.3% compared with non-Ménière’s disease samples. The results demonstrate the viability of earwax as a reporter of the presence of an otolaryngological disorder. The finding that the presence or absence of the disease can be revealed based on the concentrations of a subset of three fatty acids opens up new vistas of investigation into the possible role that fatty acid metabolism and/or dysregulation may have in Ménière’s disease.

## METHODS

**Collection of Clinical Samples.** All methods and experimental protocols described herein were reviewed by the University at Albany, State University of New York Institutional Review Board (submission #5183), and the study was deemed to be exempt because samples were considered to be discarded. As a result, no patient consent was required. All procedures were performed in accordance with relevant guidelines. Earwax was obtained from patrons at Albany ENT & Allergy Services (Albany, NY). The earwax was acquired using a standard manual removal method by trained clinicians,<sup>64</sup> thereby greatly reducing the opportunity for patient harm during the extraction. Samples were disaggregated by donor characteristics (i.e., non-Ménière’s disease diagnosis and Ménière’s disease diagnosis across age, gender, and race). Samples were blinded (i.e., no patient identifiers were provided to the analysts). The plugs were transferred to sterile containers, weighed, sealed with parafilm, and stored at

−80 °C in 20 mL glass scintillation vials (Fisher Scientific, Waltham, MA) until analysis.

**GC–MS Screening of Earwax Profile.** As previously reported, ethyl acetate extracts of earwax were prepared and screened using GC–MS.<sup>38</sup> For both the non-Ménière's disease and Ménière's disease samples, earwax plugs from multiple donors were collected (on different collection dates). Approximately 10 mg of each was individually placed into 1 dram vials (VWR, Radnor, PA). To this, 200  $\mu$ L of HPLC-grade ethyl acetate (Pharmco-Aaper, Brookfield, CT) was added. The earwax/ethyl acetate suspension was macerated using the closed end of a melting point capillary tube (VWR, Radnor, PA) and vortexed to create a more homogeneous mixture. The suspension was then transferred to an Eppendorf tube, centrifuged using a table-top system for 2 min, and 100  $\mu$ L of the supernatant was transferred to a GC vial insert (Agilent, Santa Clara, CA). A 7890B gas chromatogram and 5977B mass spectrometer (Agilent, Santa Clara, CA) coupled with a GERSTEL Multipurpose Sampler (MPS) (GERSTEL, Linthicum, MD) was used. The oven had an initial temperature of 60 °C that was held for 1 min before increasing at a rate of 10 °C/min to 100 °C. The temperature then increased at a rate of 5 °C/min until reaching 300 °C where it was held for 15 min. The column used was a DB-5MS UI (30 m, 0.25 mm I.D., 0.25  $\mu$ m) (Agilent, Santa Clara, CA), and analyses were performed in splitless mode. The inlet temperature was 250 °C; the helium flow rate was 1 mL/min; and the injection volume was 1  $\mu$ L. The mass spectrometer parameters were as follows: ionization mode was EI; ion source temperature was 230 °C;  $m/z$  range was 35–1000; and solvent delay was 4 min. Data processing was performed using MassHunter Qualitative Analysis Software (Agilent, Santa Clara, CA). Squalene was purchased from Acros (Waltham, MA). Cholesterol was purchased from Fisher Scientific (Waltham, MA). Tetradecanoic acid, hexadecanoic acid, *cis*-9-hexadecenoic acid, heptadecanoic acid, *cis*-10-heptadecenoic acid, 1-decene, 1-dodecene, 1-hexadecene, 1-octadecene, 1-tetradecene, lathosterol, and 2,4-di-*tert*-butylphenol were purchased from Sigma-Aldrich (St. Louis, MO). Pentadecanoic acid and octadecanoic acid were purchased from TCI America (Philadelphia, PA) and *cis*-9-octadecenoic acid was purchased from Oakwood Chemical (Eastill, SC). Authentic standards were prepared in ethyl acetate at a final concentration of 25  $\mu$ g/mL and analyzed using the described method. Compound identities were confirmed using retention times, fragmentation patterns of standards, and comparison of the fragmentation patterns of detected compounds to those of the 2017 National Institute of Standards and Technology (NIST) Library Database (NIST MS Search 2.3).

**Sample Preparation and Ambient Ionization Mass Spectral Analysis.** For the non-Ménière's disease samples, earwax plugs from seven individual donors were selected from seven different collection dates. Seven individuals with confirmed Ménière's disease and one with a tentative Ménière's disease diagnosis served as cerumen donors. The whole, individual plugs varied in mass from 26 to 215 mg. Approximately 10 mg from each plug was placed into a single separate 1 dram vial (VWR, Radnor, PA). To this, 200  $\mu$ L of HPLC-grade ethyl acetate (Pharmco-Aaper, Brookfield, CT) was added. The earwax/ethyl acetate suspension was macerated using the closed end of a melting point capillary tube (VWR, Radnor, PA) and vortexed to create a more homogeneous mixture.

A DART standard voltage and pressure ion source (Ion Sense, Saugus, MA) coupled to an AccuTOF high-resolution mass spectrometer (JEOL USA, Inc., Peabody, MA) with a resolving power of 6000 full width at half maximum (fwhm) and mass accuracy of 5 millimass units (mmu) was used for mass measurements. All analyses were performed using positive-ion mode under soft ionization conditions. The helium gas (Airgas, Albany, NY) flow of the DART ion source was 2.0 L/min and the gas heater temperature was set to 350 °C. The mass spectrometer settings were as follows: orifice 1: 20 V; orifice 2: 5 V; ring lens: 5 V; peaks voltage: 400 V; and detector voltage: 2000 V. Spectra were acquired within the  $m/z$  range 40–1000.

Mass spectral analysis was performed by dipping the closed end of a melting point capillary tube into the suspension and presenting the coated surface of the capillary in the open-air space between the ion source and mass spectrometer inlet. Polyethylene glycol (PEG) 600 (Sigma-Aldrich, St. Louis, MO) was used as a mass calibrant for each sample. Each replicate of a sample consisted of five measurements that were averaged. The samples were analyzed ten times to acquire ten replicates per sample. TSSPro3 software (Shrader Analytical, Grosse Pointe, MI) was used for the data processing of the mass spectra, including calibration, averaging, background subtraction, and peak centroiding. The data were stored as text files. Subsequently, using a 5 mmu tolerance, the background peaks of acetone, acetic acid, ethyl acetate, and the ethyl acetate dimer were manually removed. These peaks have the following calculated protonated monoisotopic masses: 59.0497, 61.0290, 89.0603, and 177.1127.

**Statistical Analysis.** To assess whether there were statistically significant differences between non-Ménière's disease and Ménière's disease samples, a multivariate analysis of variance (MANOVA) test was applied to the DART-HRMS spectra of the earwax of the corresponding samples using MATLAB 9.3.0, R2017b software (The MathWorks, Inc., Natick, MA). Random forest (RF) was then applied to the DART-HRMS-derived chemical profiles to discriminate between the two groups. The DART mass spectra of six non-Ménière's disease samples and six confirmed Ménière's disease samples were used to build the RF model. Mass Mountaineer software (RBC Software, Portsmouth, NH) was used for spectrum analysis, mass selection, and RF-facilitated classification and discrimination. First, a heatmap rendering of the mass spectra was generated. From the heatmap,  $m/z$  values were selected with the masses-to-features selection tool using a peak relative abundance threshold cutoff of 2% and a mass tolerance set to 5 mmu. The subset of masses that enabled accurate prediction of the presence of Ménière's disease were determined through an iterative process. The RF model was built using the monoisotopic masses 255.2324, 269.2481, and 283.2637. These three masses corresponded to the formulas  $C_{16}H_{30}O_2$ ,  $C_{17}H_{32}O_2$ , and  $C_{18}H_{34}O_2$ , respectively, and were identified to be the fatty acids *cis*-9-hexadecenoic acid, *cis*-10-heptadecenoic acid, and *cis*-9-octadecenoic acid. Model merits (i.e., accuracy, sensitivity, and precision) were then assessed. In addition, external validation against the RF model was performed by screening the mass spectra of a non-Ménière's disease sample, a seventh confirmed Ménière's disease sample, and the tentatively identified Ménière's disease sample to determine the prediction accuracy.

**Quantification of Fatty Acid Earwax Constituents.** Quantification of the three fatty acids that were found to be

essential in enabling the RF model to readily discriminate between Ménière's disease and non-Ménière's disease samples (i.e., *cis*-9-hexadecenoic acid, *cis*-10-heptadecenoic acid, and *cis*-9-octadecenoic acid) was performed by GC–MS using a 7890B gas chromatogram and a 5977B mass spectrometer (Agilent, Santa Clara, CA) coupled with a GERSTEL MPS (GERSTEL, Linthicum, MD). The column used was an HP-FFAP (30 m, 0.25 mm I.D., 0.25  $\mu$ m) (Agilent, Santa Clara, CA). The oven initial temperature was 195 °C and was increased at a rate of 5 °C/min until reaching 240 °C, where it was held for 16 min. The inlet temperature was 250 °C, the helium flow rate was 1 mL/min, and 1  $\mu$ L of sample was injected in splitless mode. The mass spectrometer parameters were as follows: the ionization mode was EI, the ion source temperature was 230 °C, the *m/z* range was 35–1000, and the solvent delay was 2 min. Data processing including automatic and manual peak integration was performed using MassHunter Qualitative Analysis Software (Agilent, Santa Clara, CA).

A calibration curve was first created using the internal standard (IS) 19-methyl eicosanoic acid (Sigma-Aldrich, St. Louis, MO). Calibrators with concentrations of 5, 10, 20, 40, 80, 100, 200 and 400  $\mu$ g/mL were prepared from a standard stock solution of 2.5 mg/mL (2500  $\mu$ g/mL) of IS in hexanes (Pharmco-Aaper, Brookfield, CT). This process was repeated twice more, and all stocks were analyzed in replicates of three. A standard curve was generated by plotting the area under the curve against the concentration.

To quantify the fatty acids, a 10 mg sample of earwax was suspended in 200  $\mu$ L of hexanes. The solution was vortexed and 100  $\mu$ L was transferred to a 2 mL Eppendorf tube and centrifuged. To further dilute the sample, 50  $\mu$ L of the supernatant was then transferred to a glass insert (Agilent, Santa Clara, CA) within a GC vial (Agilent, Santa Clara, CA) and 50  $\mu$ L of hexanes was added to create a 1:1 dilution. Finally, 5  $\mu$ L of IS at a concentration of 2100  $\mu$ g/mL was added and the sample was analyzed by GC–MS using the parameters described above. Each sample was analyzed in triplicate to ensure that any outlier area under the curve values could be removed before averaging. For one non-Ménière's disease plug, the sample was found to be too concentrated, and in this case, the sample was made using only 10  $\mu$ L of supernatant and 90  $\mu$ L of hexanes before adding the 5  $\mu$ L IS. The concentration of each fatty acid of interest was calculated using the standard curve. This was then converted to  $\mu$ g of each fatty acid per mg of the individual plug using the plug's total mass. A total of ten plugs from non-Ménière's disease donors and eight plugs from Ménière's disease donors were analyzed.

## ■ ASSOCIATED CONTENT

### SI Supporting Information

The Supporting Information is available free of charge at <https://pubs.acs.org/doi/10.1021/acsomega.3c01943>.

Additional gas chromatograms, mass spectral peak lists, random forest classification merits, external validation results, and additional fatty acid quantification details (PDF)

## ■ AUTHOR INFORMATION

### Corresponding Author

Rabi Ann Musah – Department of Chemistry, University at Albany, State University of New York, Albany, New York

12222, United States; [orcid.org/0000-0002-3135-4130](https://orcid.org/0000-0002-3135-4130);  
Email: [rmusah@albany.edu](mailto:rmusah@albany.edu)

### Authors

Allix Marie Coon – Department of Chemistry, University at Albany, State University of New York, Albany, New York 12222, United States; [orcid.org/0000-0003-3933-5804](https://orcid.org/0000-0003-3933-5804)  
Gavin Setzen – Albany ENT and Allergy Services, Albany, New York 12205, United States

Complete contact information is available at:

<https://pubs.acs.org/10.1021/acsomega.3c01943>

### Author Contributions

R.A.M. conceived of the work and designed experiments, supervised, and acquired funding for the project. A.M.C. performed the described experiments. G.S. facilitated the collection of samples and made Ménière's disease diagnoses. R.A.M. and A.M.C. drafted the manuscript.

### Notes

The authors declare no competing financial interest.

## ■ ACKNOWLEDGMENTS

The funding support of the National Institute of Deafness and Other Communication Disorders (NIDCD) through the National Institute of Health (NIH) under grant no. 1R21DC020565-01 and the National Science Foundation (NSF) under grant no. 1429329 to R.A.M. is gratefully acknowledged. We would also like to acknowledge the physicians, nurses, and staff at Albany ENT & Allergy Services for the collection of cerumen samples and Dr. Samira Beyramysoltan for helpful discussions.

## ■ REFERENCES

- (1) Chace, D. H. Mass spectrometry in the clinical laboratory. *Chem. Rev.* **2001**, *101*, 445–478.
- (2) Swiner, D. J.; Jackson, S.; Burris, B. J.; Badu-Tawiah, A. K. Applications of mass spectrometry for clinical diagnostics: The influence of turnaround time. *Anal. Chem.* **2020**, *92*, 183–202.
- (3) Crutchfield, C. A.; Thomas, S. N.; Sokoll, L. J.; Chan, D. W. Advances in mass spectrometry-based clinical biomarker discovery. *Clin. Proteomics* **2016**, *13*, 1.
- (4) Banerjee, S. Empowering clinical diagnostics with mass spectrometry. *ACS Omega* **2020**, *5*, 2041–2048.
- (5) Crutchfield, C. A.; Clarke, W. Present and future applications of high resolution mass spectrometry in the clinic. *Discoveries* **2014**, *2*, No. e17.
- (6) Diamandis, E. P. Mass spectrometry as a diagnostic and a cancer biomarker discovery tool: Opportunities and potential limitations. *Mol. Cell. Proteomics* **2004**, *3*, 367–378.
- (7) Chace, D. H.; Kalas, T. A.; Naylor, E. W. The application of tandem mass spectrometry to neonatal screening for inherited disorders of intermediary metabolism. *Annu. Rev. Genomics Hum. Genet.* **2002**, *3*, 17–45.
- (8) Hallpike, C. S.; Cairns, H. Observations on the pathology of Ménière's syndrome. *Proc. R. Soc. Med.* **1938**, *31*, 1317–1336.
- (9) Cawthorne, T.; Hewlett, A. B. Ménière's disease. *Proc. R. Soc. Med.* **1954**, *47*, 663.
- (10) Hallpike, C. S. Ménière's Disease Lecture given at Cours International de Labyrinthologie Clinique, Paris, January 15–21, 1955. *Postgrad. Med. J.* **1955**, *31*, 330–340.
- (11) Gürkov, R.; Pyykö, I.; Zou, J.; Kentala, E. What is Meniere's disease? A contemporary re-evaluation of endolymphatic hydrops. *J. Neurol.* **2016**, *263*, S71–S81.
- (12) Lopez-Escamez, J. A.; Carey, J.; Chung, W.-H.; Goebel, J. A.; Magnusson, M.; Mandalà, M.; Newman-Toker, D. E.; Strupp, M.;

- Suzuki, M.; Trabalzi, F.; et al. Diagnostic criteria for Menière's disease. *J. Vestib. Res.* **2015**, *25*, 1–7.
- (13) Conte, G.; Caschera, L.; Calloni, S.; Barozzi, S.; Di Berardino, F.; Zanetti, D.; Scuffi, C.; Scola, E.; Sina, C.; Triulzi, F. MR imaging in Menière disease: Is the contact between the vestibular endolymphatic space and the oval window a reliable biomarker? *AJNR Am. J. Neuroradiol.* **2018**, *39*, 2114–2119.
- (14) Bernaerts, A.; Vanspauwen, R.; Blaivie, C.; van Dinther, J.; Zarowski, A.; Wuyts, F. L.; Vanden Bossche, S.; Offeciers, E.; Casselman, J. W.; De Foer, B. The value of four stage vestibular hydrops grading and asymmetric perilymphatic enhancement in the diagnosis of Menière's disease on MRI. *Neuroradiology* **2019**, *61*, 421–429.
- (15) Ito, T.; Inoue, T.; Inui, H.; Miyasaka, T.; Yamanaka, T.; Kichikawa, K.; Takeda, N.; Kasahara, M.; Kitahara, T.; Naganawa, S. Novel magnetic resonance imaging-based method for accurate diagnosis of Meniere's disease. *Front. Surg.* **2021**, *8*, 671624.
- (16) van der Lubbe, M.; Vaidyanathan, A.; de Wit, M.; van den Burg, E. L.; Postma, A. A.; Bruintjens, T. D.; Bilderbeek-Beckers, M. A. L.; Dammeijer, P. F. M.; Bossche, S. V.; Van Rompaey, V.; Lambin, P.; van Hoof, M.; van de Berg, R. A non-invasive, automated diagnosis of Menière's disease using radiomics and machine learning on conventional magnetic resonance imaging: A multicentric, case-controlled feasibility study. *Radiol. Med.* **2022**, *127*, 72–82.
- (17) Hornibrook, J.; Kalin, C.; Lin, E.; O'Beirne, G. A.; Gourley, J. Transtympanic electrocochleography for the diagnosis of Ménière's disease. *Int. J. Otolaryngol.* **2012**, *2012*, 1–11.
- (18) Vlastarakos, P. V.; Vassiliou, A.; Maragoudakis, P.; Candiloros, D.; Nikolopoulos, T. Meniere's disease: Still a mystery disease with difficult differential diagnosis. *Ann. Indian Acad. Neurol.* **2011**, *14*, 12–18.
- (19) Yang, C. H.; Yang, M. Y.; Hwang, C. F.; Lien, K. H. Functional and molecular markers for hearing loss and vertigo attacks in Meniere's disease. *Int. J. Mol. Sci.* **2023**, *24*, 2504.
- (20) Chiarella, G.; Saccomanno, M.; Scumaci, D.; Gaspari, M.; Faniello, M. C.; Quaresima, B.; Di Domenico, M.; Ricciardi, C.; Petrolo, C.; Cassandro, C.; et al. Proteomics in Ménière disease. *J. Cell. Physiol.* **2012**, *227*, 308–312.
- (21) Kim, S. H.; Kim, J. Y.; Lee, H. J.; Gi, M.; Kim, B. G.; Choi, J. Y. Autoimmunity as a candidate for the etiopathogenesis of Meniere's disease: Detection of autoimmune reactions and diagnostic biomarker candidate. *PLoS One* **2014**, *9*, No. e111039.
- (22) Shew, M.; Wichova, H.; St Peter, M.; Warnecke, A.; Staecker, H. Distinct microRNA profiles in the perilymph and serum of patients with Menière's disease. *Front. Neurol.* **2021**, *12*, 646928.
- (23) Ishiyama, G.; Lopez, I. A.; Ishiyama, P.; Vinters, H. V.; Ishiyama, A. The blood labyrinthine barrier in the human normal and Meniere's disease macula utricule. *Sci. Rep.* **2017**, *7*, 253.
- (24) Di Berardino, F.; Zanetti, D. Increased urinary volumes in symptomatic Ménière's disease. *BMC Res. Notes* **2019**, *12*, 826.
- (25) Mishra, A.; Greaves, R.; Massie, J. The relevance of sweat testing for the diagnosis of cystic fibrosis in the genomic era. *Clin. Biochem. Rev.* **2005**, *26*, 135–154.
- (26) Malamud, D. Saliva as a diagnostic fluid. *Dent. Clin. North Am.* **2011**, *55*, 159–178.
- (27) Hanger, H. C.; Mulley, G. P. Cerumen: Its fascination and clinical importance: A review. *J. R. Soc. Med.* **1992**, *85*, 346–349.
- (28) Shokry, E.; de Oliveira, A. E.; Avelino, M. A. G.; de Deus, M. M.; Filho, N. R. A. Earwax: A neglected body secretion or a step ahead in clinical diagnosis? A pilot study. *J. Proteomics* **2017**, *159*, 92–101.
- (29) Barbosa, J. M. G.; Pereira, N. Z.; David, L. C.; de Oliveira, C. G.; Soares, M. F. G.; Avelino, M. A. G.; de Oliveira, A. E.; Shokry, E.; Filho, N. R. A. Cerumenogram: A new frontier in cancer diagnosis in humans. *Sci. Rep.* **2019**, *9*, 11722.
- (30) Alvord, L. S.; Farmer, B. L. Anatomy and orientation of the human external ear. *J. Am. Acad. Audiol.* **1997**, *8*, 383–390.
- (31) Petrakis, N. L.; Doherty, M.; Lee, R. E.; Smith, S. C.; Page, N. L. Demonstration and implications of lysozyme and immunoglobulins in human ear wax. *Nature* **1971**, *229*, 119–120.
- (32) Yoshiura, K.-I.; Kinoshita, A.; Ishida, T.; Ninokata, A.; Ishikawa, T.; Kaname, T.; Bannai, M.; Tokunaga, K.; Sonoda, S.; Komaki, R.; Ihara, M.; Saenko, V.; Alipov, G.; Sekine, I.; Komatsu, K.; Takahashi, H.; Nakashima, M.; Sosonkina, N.; Mapendano, C.; Ghadami, M.; et al. A SNP in the ABCC11 gene is the determinant of human earwax type. *Nat. Genet.* **2006**, *38*, 324–330.
- (33) Nitta, H.; Ikai, K. Studies on the body odor part 1. Separation of the lower fatty acids of the cutaneous excretion by paper chromatography. *Nagoya Med. J.* **1953**, *1*, 217–224.
- (34) Akobjanoff, L.; Carruthers, C.; Senturia, B. H. The chemistry of cerumen: A preliminary report. *J. Invest. Dermatol.* **1954**, *23*, 43–50.
- (35) Harvey, D. J. Identification of long-chain fatty acids and alcohols from human cerumen by the use of picolinyl and nicotinate esters. *Biomed. Environ. Mass Spectrom.* **1989**, *18*, 719–723.
- (36) Okuda, I.; Bingham, B.; Stoney, P.; Hawke, M. The organic composition of earwax. *J. Otolaryngol.* **1991**, *20*, 212–215.
- (37) Stránský, K.; Valterová, I.; Kofroňová, E.; Urbanová, K.; Zarevúcka, M.; Wimmer, Z. Non-polar lipid components of human cerumen. *Lipids* **2011**, *46*, 781–788.
- (38) Coon, A. M.; Dane, A. J.; Setzen, G.; Cody, R. B.; Musah, R. A. Two-dimensional gas chromatographic and mass spectrometric characterization of lipid-rich biological matrices - Application to human cerumen (earwax). *ACS Omega* **2022**, *7*, 230–239.
- (39) Burkhart, C. N.; Burkhart, C. G.; Williams, S.; Andrews, P. C.; Adappa, V.; Arbogast, J. In pursuit of ceruminolytic agents: A study of earwax composition. *Am. J. Otolaryngol.* **2000**, *21*, 157–160.
- (40) Shichijo, S.; Masuda, H.; Takeuchi, M. Carbohydrate composition of glycopeptides from the human cerumen. *Biochem. Med.* **1979**, *22*, 256–263.
- (41) Inaba, M.; Chung, T. H.; Kim, J. C.; Choi, Y. C.; Kim, J. H. Lipid composition of ear wax in hircismus. *Yonsei Med. J.* **1987**, *28*, 49–51.
- (42) Bortz, J. T.; Wertz, P. W.; Downing, D. T. Composition of cerumen lipids. *J. Am. Acad. Dermatol.* **1990**, *23*, 845–849.
- (43) Burkhart, C. N.; Kruge, M. A.; Burkhart, C. G.; Black, C. Cerumen composition by flash pyrolysis-gas chromatography/mass spectrometry. *Otol. Neurotol.* **2001**, *22*, 715–722.
- (44) Blackburn, P. R.; Gass, J. M.; Pinto e Vairo, F.; Farnham, K. M.; Atwal, H. K.; Macklin, S.; Klee, E. W.; Atwal, P. S. Maple syrup urine disease: Mechanisms and management. *Appl. Clin. Genet.* **2017**, *10*, 57–66.
- (45) Appley, M. G.; Beyramysoltan, S.; Musah, R. A. Random forest processing of direct analysis in real-time mass spectrometric data enables species identification of psychoactive plants from their headspace chemical signatures. *ACS Omega* **2019**, *4*, 15636–15644.
- (46) Beyramysoltan, S.; Abdul-Rahman, N.-H.; Musah, R. A. Call it a "nightshade" — A hierarchical classification approach to identification of hallucinogenic Solanaceae spp. using DART-HRMS-derived chemical signatures. *Talanta* **2019**, *204*, 739–746.
- (47) Chambers, M. I.; Osborne, A. M.; Musah, R. A. Rapid detection and validated quantification of psychoactive compounds in complex plant matrices by direct analysis in real time-high resolution mass spectrometry - Application to "kava" psychoactive pepper products. *Rapid Commun. Mass Spectrom.* **2019**, *33*, 1915–1925.
- (48) Lesiak, A. D.; Cody, R. B.; Dane, A. J.; Musah, R. A. Rapid detection by direct analysis in real time-mass spectrometry (DART-MS) of psychoactive plant drugs of abuse: The case of *Mitragyna speciosa* aka "kratom". *Forensic Sci. Int.* **2014**, *242*, 210–218.
- (49) Lesiak, A. D.; Cody, R. B.; Dane, A. J.; Musah, R. A. Plant seed species identification from chemical fingerprints: A high-throughput application of direct analysis in real time mass spectrometry. *Anal. Chem.* **2015**, *87*, 8748–8757.
- (50) Beyramysoltan, S.; Giffen, J. E.; Rosati, J. Y.; Musah, R. A. Direct analysis in real time-mass spectrometry and Kohonen artificial neural networks for species identification of larva, pupa and adult life stages of carrion insects. *Anal. Chem.* **2018**, *90*, 9206–9217.

(51) Giffen, J. E.; Rosati, J. Y.; Longo, C. M.; Musah, R. A. Species identification of necrophagous insect eggs based on amino acid profile differences revealed by direct analysis in real time-high resolution mass spectrometry. *Anal. Chem.* **2017**, *89*, 7719–7726.

(52) Hayes, J. M.; Abdul-Rahman, N.-H.; Gerdes, M. J.; Musah, R. A. Coral genus differentiation based on direct analysis in real time-high resolution mass spectrometry-derived chemical fingerprints. *Anal. Chem.* **2021**, *93*, 15306–15314.

(53) Price, E. R.; McClure, P. J.; Jacobs, R. L.; Espinoza, E. O. Identification of rhinoceros keratin using direct analysis in real time time-of-flight mass spectrometry and multivariate statistical analysis. *Rapid Commun. Mass Spectrom.* **2018**, *32*, 2106–2112.

(54) Zhang, X.; Ren, X.; Chingin, K. Applications of direct analysis in real time mass spectrometry in food analysis: A review. *Rapid Commun. Mass Spectrom.* **2021**, *35*, No. e9013.

(55) Coon, A. M.; Beyramysoltan, S.; Musah, R. A. A chemometric strategy for forensic analysis of condom residues: Identification and marker profiling of condom brands from direct analysis in real time-high resolution mass spectrometric chemical signatures. *Talanta* **2019**, *194*, 563–575.

(56) Fowble, K. L.; Shepard, J. R. E.; Musah, R. A. Identification and classification of cathinone unknowns by statistical analysis processing of direct analysis in real time-high resolution mass spectrometry-derived “neutral loss” spectra. *Talanta* **2018**, *179*, 546–553.

(57) Lesiak, A. D.; Musah, R. A.; Cody, R. B.; Domin, M. A.; Dane, A. J.; Shepard, J. R. E. Direct analysis in real time mass spectrometry (DART-MS) of “bath salt” cathinone drug mixtures. *Analyst* **2013**, *138*, 3424–3432.

(58) Zhao, Y.; Lam, M.; Wu, D.; Mak, R. Quantification of small molecules in plasma with direct analysis in real time tandem mass spectrometry, without sample preparation and liquid chromatographic separation. *Rapid Commun. Mass Spectrom.* **2008**, *22*, 3217–3224.

(59) Zhang, Y.; Zhang, W.; Xin, G.; Liu, L.; Duan, X.; Liu, C. Rapid screening of nine illicit drugs in human blood and urine by direct analysis in real-time mass spectrometry. *J. Forensic Sci. Med.* **2019**, *5*, 136–140.

(60) Lesiak, A. D.; Adams, K. J.; Domin, M. A.; Henck, C.; Shepard, J. R. E. DART-MS for rapid, preliminary screening of urine for DMAA. *Drug Test. Anal.* **2014**, *6*, 788–796.

(61) Jagerdeo, E.; Abdel-Rehim, M. Screening of cocaine and its metabolites in human urine samples by direct analysis in real-time source coupled to time-of-flight mass spectrometry after online preconcentration utilizing microextraction by packed sorbent. *J. Am. Soc. Mass Spectrom.* **2009**, *20*, 891–899.

(62) Beck, R.; Carter, P.; Shonsey, E.; Graves, D. Tandem DART<sup>TM</sup> MS methods for methadone analysis in unprocessed urine. *J. Anal. Toxicol.* **2016**, *40*, 140–147.

(63) Musah, R. A.; Lesiak, A. D.; Maron, M. J.; Cody, R. B.; Edwards, D.; Fowble, K. L.; Dane, A. J.; Long, M. C. Mechanosensitivity below ground: Touch-sensitive smell-producing roots in the shy plant *Mimosa pudica*. *Plant Physiol.* **2016**, *170*, 1075–1089.

(64) Schwartz, S. R.; Magit, A. E.; Rosenfeld, R. M.; Ballachanda, B. B.; Hackell, J. M.; Krouse, H. J.; Lawlor, C. M.; Lin, K.; Parham, K.; Stutz, D. R.; Walsh, S.; Woodson, E. A.; Yanagisawa, K.; Cunningham, E. R. Clinical practice guideline (update): Earwax (cerumen impaction). *Otolaryngol.–Head Neck Surg.* **2017**, *156*, S1–29.